

Title	Influence of surface ligands on saturation magnetization of FePt nanoparticles
Author(s)	Tanaka, Yasushi; Saita, Soichiro; Maenosono, Shinya
Citation	Applied Physics Letters, 92(9): 093117-1-093117-3
Issue Date	2008-03-05
Type	Journal Article
Text version	publisher
URL	http://hdl.handle.net/10119/7785
Rights	Copyright 2008 American Institute of Physics. This article may be downloaded for personal use only. Any other use requires prior permission of the author and the American Institute of Physics. The following article appeared in Yasushi Tanaka, Soichiro Saita, and Shinya Maenosono, Applied Physics Letters, 92(9), 093117 (2008) and may be found at http://link.aip.org/link/?APPLAB/92/093117/1
Description	

Influence of surface ligands on saturation magnetization of FePt nanoparticles

Yasushi Tanaka,¹ Soichiro Saita,² and Shinya Maenosono^{1,a)}

¹Japan Advanced Institute of Science and Technology, 1-1 Asahidai, Nomi, Ishikawa, 923-1292, Japan

²Mitsubishi Chemical Group Science and Technology Research Center, Inc., 1000 Kamoshida-cho, Aoba-ku, Yokohama, 227-8502, Japan

(Received 4 February 2008; accepted 12 February 2008; published online 5 March 2008)

The influence of organic ligands on the saturation magnetization (M_S) of chemically disordered face-centered-cubic (fcc) FePt nanoparticles (NPs) was investigated. By increasing the basicity and/or surface coverage of ligands, the M_S of fcc-phase FePt NPs decreases due to an increase in electron donation from the ligand to the Fe d bands. FePt NPs capped with 1-octanethiol or 1-dodecanethiol show larger M_S than as-synthesized NPs capped with oleic acid due to a thinning of the nonmagnetic shell. © 2008 American Institute of Physics. [DOI: 10.1063/1.2891083]

$L1_0$ -phase FePt nanoparticles (NPs) are an excellent magnetic material and, thus, have been paid much attention for their use as ultrahigh density magnetic storage media.¹ Meanwhile, superparamagnetic face-centered-cubic (fcc) FePt NPs are also expected to perform well as high-performance nanomagnets for use in medicine,²⁻⁴ because they show high magnetocrystalline anisotropy energy and high saturation magnetization (M_S) compared to superparamagnetic iron oxide (SPIO) NPs, which are the currently used nanomagnets. However, the magnetic properties of fcc-FePt NPs are strikingly different from their bulk counterpart because of various size effects. For example, the M_S of 3 nm fcc-FePt NPs capped with oleic acid (OAc) or oleylamine is approximately five times smaller than that of bulk FePt due to the nonmagnetic shell (surface dead layer) formed via electron donation from the ligands to the NPs.⁵ To exploit the superior intrinsic properties of FePt, one should understand the influence of the surface ligands on the M_S of FePt NPs to design high- M_S fcc-FePt NPs having sufficient colloidal stability.

In this letter, we chemically synthesized 9 nm fcc-FePt NPs and prepared six different NPs capped with either caprylic acid (C8Ac), lauric acid (C12Ac), 1-octanethiol (C8T), 1-dodecanethiol (C12T), 1-octylamine (C8Am), or 1-dodecylamine (C12Am) using the ligand exchange technique. Then, the M_S values of the NPs were precisely measured to investigate the influences of the chain length and functional group of the ligands on the magnetic property of FePt NPs.

FePt NPs capped with OAc were synthesized using a previously reported method^{6,7} with some modifications. The OAc groups were then converted to C8Ac, C12Ac, C8T, C12T, C8Am, or C12Am via ligand exchange. The resulting FePt NPs were characterized by transmission electron microscopy (TEM), x-ray diffraction (XRD), energy-dispersive x-ray spectroscopy (EDX), diffuse reflectance Fourier transform-infrared spectroscopy (FT-IR), CHNS elemental analysis, and superconducting quantum interference device magnetometry. The blocking temperature (T_B) was measured using zero-field-cooled (ZFC) and field-cooled (FC) measurements. The temperature sweeps were collected under a

constant field of 500 Oe. The magnetization (M - H) curve was measured as a function of the applied field at temperatures over T_B . Two samples were prepared for each ligand and the M - H measurements were carried out for these samples under the same conditions to ensure reproducibility.

Figure 1(a) shows the IR spectra of as-synthesized FePt NPs taken by FT-IR spectroscopy. The peaks at 1709, 2854, and 2924 cm^{-1} seen in the IR spectrum of the as-synthesized NPs correspond to the C=O stretching mode of the COOH group, and the symmetric and asymmetric CH_2 stretching modes of the oleyl group, respectively. No amine-derived peak was observed in the IR spectrum indicating that the dominant surface ligand was OAc, in accordance with the previous study.⁷ The inset in Fig. 1(a) shows a TEM image of the as-synthesized NPs (OAc-FePt). The mean diameter and standard deviation of the size distribution were 9 nm and 13%, respectively. EDX and XRD analyses confirmed that the average composition and the crystal structure of NPs were $\text{Fe}_{50}\text{Pt}_{50}$ and fcc phase, respectively. Figure 1(b) shows

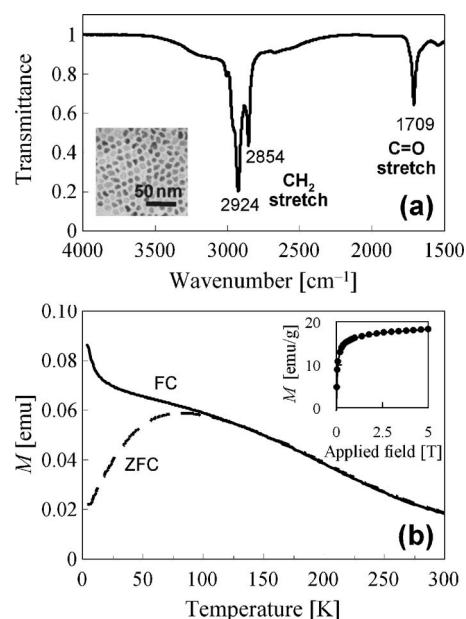


FIG. 1. (a) IR spectrum of OAc-FePt. The inset shows a TEM image of the NPs. (b) FC and ZFC magnetization vs temperature curves for OAc-FePt. The inset shows magnetization vs applied field curve measured at 160 K.

^{a)}Electronic mail: shinya@jaist.ac.jp.

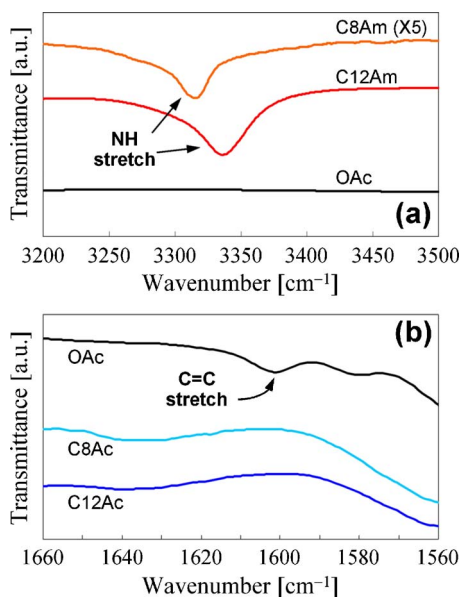


FIG. 2. (Color online) (a) IR spectra of OAc-FePt (black), C8Am-FePt (orange), and C12Am-FePt (red). (b) IR spectra of OAc-FePt (black), C8Ac-FePt (light blue), and C12Ac-FePt (blue).

the temperature dependence of magnetization for the OAc-FePt. The blocking temperature T_B was found to be about 140 K. Hence, the M - H measurements were carried out at 160 K for all samples. The inset in Fig. 1(b) shows the M - H curve of the OAc-FePt.

Figure 2(a) shows the IR spectra of C8Am-FePt and C12Am-FePt. A peak in the 3250–3400 cm^{-1} region corresponds to the N—H stretching of the amino group, indicating that the ligands were exchanged. In the cases of thiols, the S—H stretching band at 2550–2600 cm^{-1} will disappear upon chemisorption. Therefore, the surface-to-surface interparticle distances between NPs (L) were measured from TEM images. As a result, L was found to be 1.3 ± 0.4 and 2.3 ± 0.3 nm for C8T-FePt and C12T-FePt, respectively, which are approximately 1.5 times larger than the molecular lengths of the thiols, suggesting that the alkyl chains are partly interpenetrated with each other (Table I). These values are smaller than the L value of the OAc-FePt (2.5 ± 0.5 nm), indicating that the ligands were exchanged from OAc to C8T or C12T. The results of elemental analysis are summarized in Table I. In the cases of thiols and amines, the replacement rate of ligand (x) could be calculated as $x = \phi / (\phi + \phi^*)$, where ϕ and ϕ^* are the molalities of the ligands and of OAc in the sample, respectively. As shown in Table I, almost all of

TABLE I. Results of CHNS elemental and TEM analyses of FePt NPs.

Ligand	W (mg)	Composition ($\mu\text{mol}/\text{mg}$)				ϕ ($\mu\text{mol}/\text{mg}$)	L (nm)	x
		C	H	N	S			
OAc	5.87	5.4	9.6	0.0	0.0	0.27	2.5 ± 0.5	...
C8Ac	10.49	3.3	5.9	0.0	0.0	0.41	1.4 ± 0.3	...
C12Ac	6.70	5.2	9.1	0.1	0.0	0.43	2.8 ± 0.4	...
C8T	7.24	8.0	17.2	0.0	0.9	0.86	1.3 ± 0.4	0.9
C12T	5.64	7.0	14.9	0.0	0.5	0.46	2.3 ± 0.3	0.9
C8Am	9.21	3.8	7.3	0.3	0.1	0.33	1.8 ± 0.3	0.8
C12Am	11.38	3.2	6.4	0.2	0.0	0.22	2.5 ± 0.4	0.9

TABLE II. Saturation magnetization, differential magnetization, dead layer thickness, and lowering ability of magnetization of ligand.

Ligand	M_S (emu/g)	ΔM_S (emu/g)	δ (nm)	ζ (emu/ μmol)
OAc	19.5	55.5	1.63	0.206
C8Ac	19.6 ± 0.4	55.4 ± 0.4	1.62	0.135 ± 0.001
C12Ac	15.3 ± 2.8	59.7 ± 2.8	1.85	0.139 ± 0.007
C8T	20.8 ± 0.1	54.2 ± 0.1	1.57	0.063 ± 0.000
C12T	22.3 ± 0.1	52.7 ± 0.1	1.50	0.115 ± 0.000
C8Am	21.0 ± 3.1	54.0 ± 3.1	1.56	0.164 ± 0.009
C12Am	20.4 ± 2.0	54.6 ± 2.0	1.58	0.248 ± 0.009

the OAc groups were found to be replaced by either thiols or amines ($x \geq 0.8$).

On the other hand, in the cases of saturated fatty acids, it was difficult to clearly confirm the ligand exchange reaction using FT-IR spectroscopy, even though the C=C stretching peak, which was weakly observed in the OAc-FePt at ~ 1600 cm^{-1} , disappeared in the IR spectra of the C8Ac-FePt and C12Ac-FePt, as shown in Fig. 2(b). It was also difficult to estimate x by elemental analysis because these NPs do not have a characteristic element, such as N or S, in the molecule. However, L was found to be ligand-dependent. The values of L were 1.4 ± 0.3 and 2.8 ± 0.4 nm for the C8Ac-FePt and C12Ac-FePt, respectively (Table I). Based on these results, we could conclude that almost all of the OAc groups were replaced by C8Ac or C12Ac.

A significant difference in M_S was observed among the NPs capped with different ligands, as shown in Table II. Since the M_S value of bulk FePt was reported to be 75 emu/g,⁸ the remarkable reduction in M_S is possibly due to the surface dead layer effect. The dead layer thickness (δ) is estimated as $\delta = D_p [1 - (M_S/M_{S,\text{bulk}})^{1/3}] / 2$, where D_p and $M_{S,\text{bulk}}$ are the mean diameter of NPs and M_S of bulk FePt, respectively (Table II). The C12T-FePt and C12Ac-FePt have the thinnest ($\delta = 1.5$ nm) and thickest ($\delta = 1.85$ nm) dead layers, respectively. One explanation for the origin of the difference in M_S among NPs capped with various ligands can be interpreted as the difference in the electron donation ability of the ligands to the Fe d bands. A spin-polarized density functional calculation predicts that the lowering of the atomic magnetization of Fe takes place when charge is transferred to the surface Fe sites from oleylamine.⁵ The lowering ability of magnetization of the ligand (ζ) can be defined as $\zeta = \Delta M_S / \phi$ where $\Delta M_S = M_{S,\text{bulk}} - M_S$ is the differential magnetization (Table II). The value of ζ tends to increase with increases to the alkyl chain length of the ligand regardless of the functional group. This behavior would be explained by the chain-length effect of hydrocarbons on the electron-donating ability.

On the other hand, ζ decreases in the order of alkyllamine, fatty acid, and alkanethiol, when the chain length is the same. The basicity constant pK_b of typical aliphatic amines, fatty acids, and alkanethiols are ~ 3 , 9, and 4, respectively. Hence, it is intelligible that amines exhibit the largest ζ . On the contrary, it is unaccountable that thiols have the smallest ζ despite having the second-strongest basicity. In general, thiols are known to form weaker bonds with iron oxides than carboxylic acids,⁹ though thiols do strongly bind to Pt. Thus, a significant fraction of thiols is considered to adsorb on Pt sites on the surface of NPs. The ligands adsorb-

ing on Pt sites would influence magnetic properties of NPs much less than the ligands binding to Fe sites. Hence, the C12T-FePt has thinner dead layer than the C12Ac-FePt. That is, δ presumably depends not only on the basicity of the ligand but also on the number of Fe-ligand binding sites. Further study will be necessary to unravel the detailed mechanism of the formation of the dead layer. Nevertheless, we found that the M_S value of FePt NPs can be improved by exchanging the surface ligands from OAc to alkanethiols. Additionally, we also found that C8T has the smallest ζ value among all ligands used in the present study, although δ of C12T-FePt is the smallest, because the surface coverage of C8T is almost twice as large as that of C12T.

In conclusion, the influence of surface ligands on the M_S of fcc-FePt NPs was investigated. The M_S of NPs capped with C8T and C12T were found to be 7% and 14% higher than that of OAc-FePt, respectively. High- M_S fcc-FePt NPs can be obtained by capping the surface of the NPs with high-

pK_b ligands and/or by reducing the number of Fe-ligand binding sites.

This work is supported by a Grant for Industrial Technology Research Program in 2006 from New Energy and Industrial Technology Development Organization (NEDO) of Japan.

¹S. Sun, C. B. Murray, D. Weller, L. Folks, and A. Moser, *Science* **287**, 1989 (2000).

²S. Maenosono and S. Saita, *IEEE Trans. Magn.* **42**, 1638 (2006).

³J. S. Choi, Y. W. Jun, S. I. Yeon, H. C. Kim, J. S. Shin, and J. Cheon, *J. Am. Chem. Soc.* **128**, 15982 (2006).

⁴C. J. Xu and S. H. Sun, *Polym. Int.* **56**, 821 (2007).

⁵X. W. Wu, C. Liu, L. Li, P. Jones, R. W. Chantrell, and D. Weller, *J. Appl. Phys.* **95**, 6810 (2004).

⁶S. Saita and S. Maenosono, *Chem. Mater.* **17**, 3705 (2005).

⁷S. Saita and S. Maenosono, *Chem. Mater.* **17**, 6624 (2005).

⁸T. Klemmer, D. Hoydick, H. Okumura, B. Zhang, and W. A. Soffa, *Scr. Metall. Mater.* **33**, 1793 (1995).

⁹G. Kataby, T. Prozorov, Y. Koltypin, H. Cohen, C. N. Sukenik, A. Ulman, and A. Gedanken, *Langmuir* **13**, 6151 (1997).